科技部補助專題研究計畫成果報告
期末報告

電位依賴型鈉離子電流在藍斑核正腎上性素神經元節律性自發放電行為之探討(第 3 年)

計 畫 類 別 ： 個別型計畫
計 畫 編 號 ： NSC 100-2320-B-040-010-MY3
執 行 期 間 ： 102 年 08 月 01 日至 103 年 07 月 31 日
執 行 單 位 ： 中山醫學大學生物醫學科學學系（所）

計 畫 主 持 人 ： 楊琇雯
共 同 主 持 人 ： 閔明源
計畫參與人員： 碩士班研究生-兼任助理人員：吳芮妮
大專生-兼任助理人員：連玉慧
大專生-兼任助理人員：李宣萱

報 告 附 件 ： 出席國際會議研究心得報告及發表論文

處 理 方 式 ：
1.公開資訊：本計畫涉及專利或其他智慧財產權，2 年後可公開查詢
2.「本研究」是否已有嚴重損及公共利益之發現：否
3.「本報告」是否建議提供政府單位施政參考：否

中 華 民 國 103 年 11 月 10 日

中文摘要： 藍斑核的神經元投射到大腦許多的區域；他們是前腦正腎上腺性素主要的來源，已知正腎上腺性素在許多知覺功能上扮演重要的角色，包括睡眠清醒週期、警覺、學習與記憶、痛覺與大腦代謝。因此，探討藍斑核神經元的調節對於瞭解藍斑核-正腎上腺性素系統與大腦功能如何被調節是必須的。這裡我們報告一種持續電壓依賴型鈉離子電流可能是藍斑核神經元產生自主性放電的主要因素。在控制組與加入 1 mM 河豚激素(TTX)組，我們紀錄藍斑核神經元對應於一個電壓坡道從 30 mV 至-100 mV(斜率＝20 mV/s)其細胞膜電流的改變；從控制組中扣除加入 TTX 組，產生一種持續電壓依賴型鈉離子電流(INaP)，INaP 的活化閾值範圍與最大振幅分別為-50 至-60 mV 及-103±16 pA (n=12 細胞)。INaP 的活化曲線依據波茲曼公式計算，得知活化斜率與半-活化電壓分別為 6.8±0.8 及-24±1.5 mV。利用非侵入性膜電位記錄，可在不影響神經細胞的離子成份下，測得細胞膜電位(Vm)，17 個藍斑核細胞的平均膜電位為-51±1.5 mV。其中 10 個細胞不會產生自主性放電，其平均膜電位為-54±1.3 mV；另外 7 個細胞會產生自主性放電，其平均膜電位為-47±1.7 mV。這些結果顯示膜電位與 INaP 的活化閾值是相似。綜合以上結果得知 INaP 的高活化斜率導致藍斑核神經元可以自我產生放電。電流嵌定記錄實驗顯示大部份的藍斑核神經元在閾值膜電位以下有電壓波動的情形，此種現象可被 connexin 阻斷劑 (carbenoxolone)抑制，顯示電壓波動是由於臨近細胞正在放電，其電流經 gap junction 流入正在記錄的細胞所產生。利用 tyrosine hydroxylase 與 Nav1.6 抗體，進行光學顯微鏡免疫組織化學染色，以觀察藍班核正腎上性素神經元在白天與晚上其 Nav1.6 離子通道的表現量是否有所不同。我們發現，在白天 32±6 %藍班核正腎上性素神經元有表現 Nav1.6；在晚上則有 46±13%藍班核正腎上性素神經元有表現 Nav1.6。這些結果顯示電壓波動使正在記錄的藍斑核細胞能夠產生局面的放電現象，並且 Nav1.6 離子通道在睡眠與清醒周期中，對於調控藍班核正腎上性素神經元動作電位放射頻率上扮演重要的角色。

中文關鍵詞： 藍斑核,日週期性,自發性放電,持續型電位依賴型鈉離子電流,Nav1.6,河豚素

英文摘要： Locus coeruleus (LC) neurons have widely projections to various areas of brain； they provide the forebrain the major supply of norepinephrine which is well known to play important roles in many cognitive functions, including sleep-wake cycle, alertness

attention, learning and memory, pain, and brain metabolism. Accordingly, investigating the regulation of LC neurons is essential to understand how LC-NE system associated brain functions are regulated. Here We reported the persistent voltage-gated sodium current (INaP) could be a major player for generating spontaneous firing in LC neurons. We recorded membrane currents responded to a voltage-ramp from 30mV to -100mV (slope = 20 mV/s) in control and in the presence of 1 贡M tetrodotoxin (TTX) in LC neurons； subtracting recording in TTX from that in control condition yielded INaP, the range of activation threshold and peak amplitude of which were about -50 to -60 mV and -103± 16 pA (n = 12 cells), respectively. The activation curve of INaP was fitted with one state Boltzmann’s equation with estimated activation slope and half-activation voltage being 6.8 ± 0.8 and -24 ± 1.5 mV, respectively. By using noninvasive membrane potential measurement to estimate resting membrane potential (Vm) without interrupting ion compositions of the recorded neurons, the averaged Vm from 17 LC neurons was -51± 1.5 mV, 10 of them whose Vm is -54 ± 1.3 mV showed no spontaneous firing and the 7 of them with estimated Vm= -47 ± 1.7 mV could fire spontaneously. These results show that Vm and activation threshold of INaP in LC neurons are about the same value. This feature together with the high activation slope of INaP could allow the self-generation of AP in LC neurons. In current clamp recording, most LC neurons showed sub-threshold voltage-oscillation, which was blocked by connexin blocker, carbenoxolone, showing the activity was generated by action currents of discharging neighboring cells flowing through gap junctions. By using antibodies against TH and Nav1.6 to examine the expression of Nav1.6 in the LC NAergic neurons at day and night time, we found that the percentage of examined LC NAergic neurons showing Nav1.6 was 32±6 % at daytime and 46±13% at nighttime. These results suggest that voltage-oscillation enable the generation of phasic firing in recorded LC neuron, and Nav1.6 may play an important role in the

regulation of firing rate of LC NAergic neurons during sleep and wake cycles.

英文關鍵詞： Locus coeruleus,circadian rhythm, spontaneous firing,persistent voltage-gated sodium current,Nav1.6, TTX

Abstract

Locus coeruleus (LC) neurons have widely projections to various areas of brain; they provide the forebrain the major supply of norepinephrine which is well known to play important roles in many cognitive functions, including sleep-wake cycle, alertness attention, learning and memory, pain, and brain metabolism. Accordingly, investigating the regulation of LC neurons is essential to understand how LC-NE system associated brain functions are regulated. Here We reported the persistent voltage-gated sodium current (I_{NaP}) could be a major player for generating spontaneous firing in LC neurons. We recorded membrane currents responded to a voltage-ramp from 30mV to -100mV (slope = 20 mV/s) in control and in the presence of 1 mM tetrodotoxin (TTX) in LC neurons; subtracting recording in TTX from that in control condition yielded I_{NaP}, the range of activation threshold and peak amplitude of which were about -50 to -60 mV and -103± 16 pA (n = 12 cells), respectively. The activation curve of I_{NaP} was fitted with one state Boltzmann's equation with estimated activation slope and half-activation voltage being 6.8 ± 0.8 and -24 ± 1.5 mV, respectively. By using noninvasive membrane potential measurement to estimate resting membrane potential (V_m) without interrupting ion compositions of the recorded neurons, the averaged V_m from 17 LC neurons was -51± 1.5 mV, 10 of them whose Vm is -54 ± 1.3 mV showed no spontaneous firing and the 7 of them with estimated Vm= -47 ± 1.7 mV could fire spontaneously. These results show that Vm and activation threshold of I_{NaP} in LC neurons are about the same value. This feature together with the high activation slope of I_{NaP} could allow the self-generation of AP in LC neurons. In current clamp recording, most LC neurons showed sub-threshold voltage-oscillation, which was blocked by connexin blocker, carbenoxolone, showing the activity was generated by action currents of discharging neighboring cells flowing through gap junctions. By using antibodies against TH and $Na_v1.6$ to examine the expression of $Na_v1.6$ in the LC NAergic neurons

at day and night time, we found that the percentage of examined LC NAergic neurons showing $Na_v1.6$ was 32±6 % at daytime and 46±13% at nighttime. These results suggest that voltage-oscillation enable the generation of phasic firing in recorded LC neuron, and $Na_v1.6$ may play an important role in the regulation of firing rate of LC NAergic neurons during sleep and wake cycles.

Introduction

The locus coeruleus (LC), a nucleus of tightly packed noradrenergic (NAergic) neurons, locates in the rostral dorsolateral pontine tegmentum (Swanson, 1976; Foote et al., 1983). LC is important in a variety of cognitive functions, including sleep-wake cycle, alertness attention, learning and memory, pain and brain metabolism (Aston-Jones, 2005). The NAergic LC neurons fire action potential spontaneously with distinct phasic and tonic modes, which result in different pattern of noradrenaline release (Aston-Jones et al., 1980; Florin-Lechner et al., 1996). The phasic discharge is characterized by brief 10-20 Hz bursts of two three action potentials that is often, but not always, followed by a sustained suppression of spontaneous activity (200-500 ms) (Akaike, 1982; Aston-Jones and Bloom, 1981b Clayton et al., 2004). Phasic bursts are elicited by novel or salient polymodal sensory stimuli as well as top-down decision- and response-related signals from prefrontal cortical regions (Aston-Jones and Bloom, 1981b, 2005a, b; Berridge and Waterhouse, 2003). The tonic activity is exemplified by stochastic discharge across a range of relatively slow rates (0.1-5.0 Hz). Increasing tonic rates are coarsely related to arousal levels within the sleep/waking continuum (Aston-Jones and Bloom, 1981a; Berridge and Waterhouse, 2003; Foote et al., 1980; Hobson et al., 1975), but during waking, these intermediate rates are more subtly related to goal-directed task flexibility (Aston-Jones et al., 1997, 2005b). Examinating of the spontaneous discharge of NAergic LC neurons during the sleep-wake cycle in behaving

rats and monkeys showed that activity varied with stage of sleep-wake cycle, such that firing was most rapid during waking (2 Hz), slower during slow-wave sleep (1 Hz), and virtually absent during paradoxical sleep (Hobson et al., 1975; Aston-Jones and Bloom, 1981a). The mechanisms underlying these changes have yet to be fully elucidated, and a starting point to which is to understand how spontaneous firing, and hence the pacemaking behavior, of LC neurons is generated.

One candidate membrane current that drives spontaneous activity of LC neurons has been the TTX-sensitive, voltage-dependent persistent sodium current ($I_{NaP,}$) which is characterized by its low voltage threshold (substhreshold) for activation and slow inactivation (Pennartz et al., 1997; Kononenko et al., 2004). Although it is very small compared to the transient sodium current that contributes to the rising phase of an action potential, I_{NaP} greatly influences the frequency and pattern of firing by producing a regenerative depolarizing current in the voltage range between the resting potential and spike threshold (Carter et al., 2012). In many neurons, I_{NaP} has been reported to drive pacemaking behavior (Bevan and Wilson, 1999; Del Negro et al., 2002), promote bursting (Azouz et al., 1996; Williams and Stuart, 1999), generate and amplify subthreshold electrical resonance (Gutfreund et al., 1995; D'Angelo et al., 1998), and promote theta-frequency oscillations (White et al., 1998; Hu et al., 2002). There are nine recognized members of the voltage-gated Na^+ channel family (VGSC; $Na_v1.1$-$Na_v1.9$). Of these, $Na_v1.1$, $Na_v1.2$, $Na_v1.3$ and $Na_v1.6$ are highly (but not exclusively) expressed in the central nervous system (CNS), whereas $Na_v1.7$, $Na_v1.8$, and $Na_v1.9$ demonstrate a more restricted expression pattern in autonomic and sensory neurons of the peripheral nervous system (PNS). The $Na_v1.6$ subtype is also highly expressed in the PNS where it is enriched at the nodes of Ranvier of myelinated axons and contributes to salutatory conduction (Caldwell et al., 2000).

Since the relative contribution of the persistent sodium channels to spontaneous firing in NAergic LC neurons is yet to be fully established, in the present study we aimed to characterize (I_{NaP}) in LC neurons. Using current-clamp and voltage-clamp recordings, we quantified TTX-sensitive membrane current that flows during inter-spike interval. By immunohistochemistry staining, we determined whether the expression of $Na_v1.6$ subtype is different during wakefulness and sleep. Our results suggest that I_{NaP} could enhance voltage-oscillation and the generation of phasic firing in recorded LC neurons, and $Na_v1.6$ is critical ion channel for the regulation of the neuronal firing pattern in the wake-sleep cycle.

.

Materials and Methods

Preparation of brain stem slices

The use of animals in this study was in accordance with the rules for animal research of the Ethical Committee of the National Science Council in Taiwan. Every effort was made to minimize the number of animals used and their suffering. Sprague-Dawley rat pups of both sexes and aged 10-13 days were used in this study. Sagittal brainstem slices (300 μm) containing LC area were cut with a vibroslicer (Dosaka, Tokyo, Japan). Slicing was perform in ice-cold artificial cerebrospinal fluid (ACSF) containing (in mM) NaCl 119, KCl 2.5, $MgSO_4$ 26.2, $NaHCO_3$ 1, $Na_2H_2PO_4$ 2.5, $CaCl_2$ 2.5 and glucose 11, with the pH adjusted to 7.4 by gassing with 95% O_2/5% CO_2. The slices were kept in an interface-type chamber at room temperature (25-26 °C) for at least 90 min to allow recovery before start of recording.

Electrophysiology

Slices were transferred to an immersion-type recording chamber mounted on an upright microscope (BX51WI; Olympus Optical, Tokyo, Japan) and continuously

perfused with oxygenated ACSF at 2-3 ml/min. Neurons were viewed using Nomarski optic. The patch pipettes, pulled from borosilicate glass tubing (1.5 mm outer diameter, 0.32 mm wall thickness, Warner Instruments, Hamden, CT), had a resistance of 3-5 MΩ when filled with internal solution consisting of (in mM) 131 K-gluconate, 20 KCl, 10 HEPES, 2 EGTA, 8 NaCl, 2 ATP, and 0.3 GTP; pH adjusted to 7.2 with KOH. Recordings were made at 33-35°C in either cell attached or whole-cell configuration with a patch amplifier (Multiclamp 700 B; Axon Instruments Inc.; Union City, CA, USA). For current-clamp recording, the bridge was balanced and neurons were only accepted for further study if the membrane potential (Vm) was at least -45 mV without applying a holding current and the action potential (AP) was able to overshoot 0 mV. For voltage-clamp recording a voltage step of 5 mV was applied at about 0.1 Hz throughout the recording to monitor serial resistances and the data were discarded if the values varied by more than 20 % of the original value, which was usually less than 20 MΩ. The cell-attached was made in voltage-clamp mode with pipette voltage set at 0 mV. Signals were low-pass filtered at a corner frequency of 2 kHz and digitized at 10 kHz using a Micro 1401 interface running Signal or Spike2 software (Cambridge Electronic Design, Cambridge, UK), respectively, for episode-based capture or continuous recording. All data are presented as the mean ± standard error of the mean (SEM) and were compared using the paired *t* test or non-parameter student *t* test. The criterion for significance was a p value < 0.05.

All chemicals used to prepared ACSF and pipette solution preparation were from Merck (Frankfurt, German); picrotoxin (Ptx), strychnine, kynurenic acid and biocytin were from Sigma (St. Louis, USA); DL-2-amino-5-phosphonopentanoic acid (APV), 6,7-dinitroquinoxaline-2,3-dione (DNQX), tetrodotoxin (TTX) were from Tocris-Cookson (Bristol, UK).

Filling of recorded neurons with biocytin and histology

The recorded neurons were filled by passive diffusion of biocytin from the patch pipette during the recording period. After recording, the brain slice were transferred to 4% paraformaldehyde (Merck, Frankfurt, Germany) in 0.1 M phosphate buffer (PB), pH 7.4, for fixation overnight at 4°C, then were subjected to histological procedures for visualization of biocytin-filled neurons without further sectioning. Briefly, the slices were incubated for 1 h at room temperature in 0.3% Triton X-100 in phosphate-buffered saline (PBST) containing 10% normal goat serum, then in 2% bovine serum albumin overnight at 4°C with a mixture of AMCA-avidin D (dilution: 1/250; Vector Laboratories, Burlingame, CA, USA) and a monoclonal mouse antibody against rabbit tyrosine hydroxylase (TH) (dilution: 1/1300; Chemicon, Temecula, CA, USA) in PBST. The slices were then incubated for 2 h at room temperature with FITC-conjugated goat anti-rabbit IgG (Jackson, PA, USA). The slices were washed at least 3 times (10 min per wash) with TPBS between incubation steps. Biocytin-filled neurons were examined for binding of anti-TH antibodies and photographed on an Olympus BX-50 fluorescent microscope (Olympus Optical Co., Ltd., Tokyo, Japan).

Immunocytochemical Tissue Processing

The use of animals in this study was in accordance with the rules for animal research of the Ethical Committee of the National Science Council in Taiwan. Thirteen C57BL6 female mice were deeply anesthetized with trichloroacetaldehyde monohydrate (10%) and perfused through the cardiovascular system with normal saline, followed by 4% paraformaldehyde in 0.1 M phosphate buffer (PB), pH7.4 (AM group: six were perfused at 10:30 AM; PM group: seven were perfused at 10:30 PM). The brain were then rapidly removed and placed in the same fixative at 4°C for 3-4 hr and washed overnight

at 4°C with PB. Serial sagittal sections containing LC and surrounding regions were cut with a cryostate (LEICA CM3050 S) at the thickness of 10 μm. Sections were incubated with 0.3% sodium borohydride in PB for 50 min antigen retrieval. Following a 10 min wash with PB and TPBS (0.3% Triton X-100 in phosphate-buffered saline containing), the sections were treated with 3% H2O2 in 0.1 M PB to quench endogenous peroxidase activity. After rinses in 0.1 M PB and TPBS, the sections were incubated in TPBS containing 2% bovine serum albumin (BSA) and 10% normal goat serum (NGS) for 1 hr to reduce non-specific binding of the antibodies. The sections were then incubated overnight at 4°C with either rabbit anti- tyrosine hydroxylase (TH) antibodies (dilution: 1/3000, Millipore) or rabbit anti-$Na_v1.6$ antibody (dilution: 1/50, Alomone Lab). After rinsed with PBS, the sections were incubated for 1 hr with biotinylated anti-rabbit IgG antibody diluted 1/100, after further rinses with PBS, were incubated for 1 hr with avidin-biotin peroxidase complex (ABC, Vector Laboratories, Burlingame, CA). Following rinsing in PBS and in PB, the sections were immersed in 0.05% diaminobenzidine (DAB, Sigma) containing 0.01% H_2O_2 in PB for 10 min. The reaction was terminated by extensive washes in PB. As a specificity control for non-specific binding, sections were incubated in TPBS in the absence of primary antibodies. The results of staining were examined and photographed on an Olympus BX-50 microscope (Olympus Optical Co., Ltd., Tokyo, Japan).

Data Analysis

To examine the percentage of LC NAergic neurons expressing $Na_v1.6$, x40 photomicrographs from 2-7 pairs of adjacent serial sections from 13 sagittally sectioned brains (six were from the AM group; seven were from the PM group) were taken. All data are expressed as the man±standard error of the mean; Mann-Whitney *U* test was used for statistical comparison.

Results and Discussions

Recording of LC neurons

Under Nomarski microscopy video at low magnification, LC was identified as transparent long-oval area located rostral to the floor of the 4th ventricle and beneath the superior cerebellar peduncle (Fig. 1A). At high magnification, numerous large neurons with soma diameter of ~25 μm could be identified and were recorded (Fig. 1A). Initially, we filled recorded neurons with biocytin and confirmed that they were immunoreactive (ir) to anti-TH antibody, thereby the NAergic (Fig. 1A). The recorded TH-ir neurons spontaneously fired action potential (AP) in most cases with a mean firing rate of ~ 0.3 Hz. Additionally, there was prominent membrane-voltage oscillation at 3.5 ±0.7 Hz (see asterisks in Fig. 1B) in most recorded LC neurons, with APs usually occurring at their peaks. Since it has been reported that NAergic LC neurons are electrically coupled (Ishimatsu and Williams 1996; Ballantyne et al., 2004), these voltage oscillation were likely due to the flow of AP currents through the gap junctions of the connected discharging NAergic neurons. In support of this speculation, these events of membrane currents oscillations recorded in voltage clamp recording (Vm = -50 mV) were completely abolished by perfusion of slices with 200 μM carbenoxolone, a gap junction blocker, in condition in which both excitatory and inhibitory postsynaptic currents (EPSCs) were blocked by addition of 5 mM kynurenic acid, 0.1 mM picrotoxin and 1 μM strychnine into the bath medium (Figure 1C). In line with recording with other pontine NAergic neurons (Min et al, 2008, 2010), TH-ir neurons in LC also showed voltage-dependent delay in firing APs, possibly caused by A-type potassium current, upon injection of hyperpolarizing and depolarizing currents pulses (Fig. 1D). Taken these features together, we considered that the recorded TH-ir neurons were NAergic LC neurons and referred them simply as LC neurons.

A total number of 58 LC neurons were recorded with current clamp mode. Based on their firing characteristics, the recorded LC neurons were be grouped into two major subtypes; the phasic firing and regular firing, which accounted for 48 % (28/58) and 52% (30/58) of the 58 recorded LC neurons, respectively. We observed a significant difference in the mean amplitude and frequency voltage-oscillations between the two groups of LC neurons. The mean amplitude and frequency of phasic firing group were, respectively, 65±8.0 pA, and 1.5±0.1 Hz, which were significantly larger than that of regular firing group (Fig. 2A, B), amplitude: 12±2.2 pA ($p<0.01$, Mann-Whiney *U*-test), frequency: 0.8±0.2 Hz ($p<0.01$, Mann-Whiney *U*-test). The gap-junction mediated voltage-oscillations appeared to have significant impact to the firing mode; shown in Figure 2C, is a typical LC neuron of phasic firing group, the firing pattern of which shifted to regular firing upon application of 200 μM carbenoxolone to inhibit the function of gap junction (voltage-oscillations).

Noninvasive measurements of membrane potential from cell-attached recordings

A general difficulty in measuring membrane potential in physiological condition has been the dialysis of intracellular ion contents by the pipette solution. To avoid this technical error, we employed noninvasive measurements of membrane potential. This method takes advantage of the high density of voltage-dependent K^+ channels on the membrane of excitable cells. By assuming the intracellular [K^+] of LC neurons being 131 mM and using pipette solution of the same K^+ concentration, the equilibrium potential of K^+ for membrane patch inside recording pipette would be 0 mV. Accordingly, physiological membrane potential could be measured by recording reversal potential of K^+ current evoked by activating voltage-dependent K^+ channels inside the path membrane with a voltage ramp in cell-attached configuration (Khaliq

and Bean, 2010; Verheugen et al., 1995; 1999). Figure 3A shows example of a typical experiment in which 1 μM TTX was added into bath medium to block spontaneous firing; as can be seen, application of voltage ramp +100 mV to -100 mV to the patch pipette evoked outward membrane current that was reversed at ~-50 mV. After correction for "leak current" by linear fit of membrane current to pipette voltage raging from +84 to +40 mV, extrapolating the linear fit revealed reversal potential of evoked K^+ current, therefore the physiological membrane potential, at the point where the liner fit crosses the membrane current (see arrow in Fig. 3A). Figure 3B shows summarized results, the averaged physiological membrane potential measured by this method from 17 LC neurons was -51.4±1.3 mV (n=17; Fig. 3B). This measurement is about the same as membrane potential measured by whole-cell recording when spontaneous APs were blocked by TTX (-51.2±1.2 mV; Fig. 3B).

Steady-state subthreshold sodium currents

We next characterized I_{NaP} of LC neurons. Figure 4A shows the currents elicited by 10 mV/s ramp from +30 mV to -100 mV in normal condition and subsequent application of 1 μM TTX into the bath medium. As can be seen the inhibition of membrane currents by TTX. Subtracting membrane currents recording in TTX application from that in normal condition yielded I_{NaP}. Figure 4B shows voltage-dependent activation of I_{NaP} and Figure 4 C shows the converted voltage-dependent I_{NaP} conductance, which were collected results from 12 LC neurons. The activation threshold for was about -60 mV, bellow the physiological membrane potential of LC neurons. The averaged maximal steady-state conductance of I_{NaP} was 1.3±0.2 nS, the half activation and slope factor estimated from Bolztman fit to the data was -24.4±1.5 mV and 6.6±0.7 mV, respectively.

Immunoreactivity of Na $_v$1.6

Immunoreactivities for both of TH and Na $_v$1.6 were revealed in neuronal cell bodies. When evaluated by light microscope, a profile was judged as being immunolabelled only when it was clearly darker than the lightly stained elements in the surrounding neuropil. Cells were accepted as double-labeled only if they were strongly labeled with both antisera.

To quantify the percentage of LC NAergic neurons with expression of Na $_v$1.6 at AM and PM, we double stained sections with antibodies against TH (tyrosine hydroxylase) and Na $_v$1.6. The percentage of LC NAergic neurons showing $Na_v1.6$ was 32±6 % at AM and 46±13% at PM ($p<0.05$, Mann-Whitney *U* test) (Fig. 5).

In conclusions, our results show that LC neurons express I_{NaP} that has activation threshold below the resting membrane potential. This observation strongly suggests that I_{NaP} could be the most important player in spontaneous firing of LC neurons, and $Na_v1.6$ may play an important role in the regulation of firing rate of LC NAergic neurons during sleep and wake cycles.

In support of this argument, our recent experiments showed that application of selective I_{NaP} inhibitor, riluzole, suppressed spontaneous firing of the LC neurons. We also observe possible interplay between gap junction and I_{NaP}, as there is a correlation between voltage-oscillations and firing pattern of LC neurons. We consider that the above results from the past year of study have characterized the basic properties of I_{NaP} and its role in driving spontaneous firing of LC neurons. We believe these results will not only provide new insight into how I_{NaP} control firing pattern of LC neurons but also a identification of molecular substrate that is responsible to NE-seretonin associated disorder, abnormal behavior in early chronic SSRI exposure.

References

Akaike T. (1982) Periodic bursting activities of locus coeruleus neurons in the rat. Brain Res. 239: 629-633.

Aston-Jones G (2005) Brain structures and receptors involved in alertness. Sleep Med 6 suppl 1: S3-S7.

Aston-Jones G, Bloom FE (1981a) Activity of norepinephrine-containing locus coeruleus neurons in behaving rats anticipates fluctuations in the sleep-waking cycle. J Neurosci 1: 876-886.

Aston-Jones G, Bloom FE (1981b) Norepinephrine-containing locus coeruleus neurons in behaving rats exhibit pronounced responses to non-noxious environmental stimuli. J Neurosci 1: 887-900.

Aston-Jones G, Cohen JD. (2005a) Adaptive gain and the role of the locus coeruleus-norepinerphine system in optimal performance. J. Comp. Neurol. 493: 99-110.

Aston-Jones G, Cohen JD. (2005b) An integrative theory of locus coeruleus-norepinephrine function: adaptive gain and optimal performance. Annu. Rev. Neurosci. 28: 403-450.

Aston-Jones G, Rajkowski J, Kubiak P. (1997) Conditioned responses of monkey locus coeruleus neurons anticipate acquisition of discriminative behavior in a vigilance task. Neuroscience 80: 697-715.

Aston-Jones G, Segal M, Bloom FE. (1980) Brain aminergic axons exhibit marked variability in conduction velocity. Brain Res. 195: 215-222.

Azouz R, Jensen MS, Yaari Y. (1996) Ionic basis of spike afterdepolarization and burst generation in adult rat hippocampal CA1 pyramidal cells. J. Physiol. 492: 211-223.

Ballantyne D, Andrzejewski M, Mückenhoff K, Scheid P (2004) Rhythms, synchrony and electrical coupling in the locus coeruleus. Respir Physiol Neurobiol **143**: 199-214.

Berridge CW, Waterhouse BD. (2003) The locus coeruleus-noradrenergic sysem: modulation of behavioral state and state-dependent cognitive processes. Brain Res. Rev. 42: 33-84.

Bevan MD, Wilson CJ. (1999) Mechanisms underlying spontaneous oscillation and rhythmic firing in rat subthalamic neurons. J. Neurosci. 19: 7617-7628.

Caldwell JH, Schaller KL, Lasher RS, Peles E, Levinson SR (2000) Sodium channel Na(v)4.6 is localized at nodes of ranvier, dendrites, and synapses. Proc Natl Acad Sci USA 97: 5616

Carter, BC, Giessel AJ, Sabatini BL, Bean BP. (2012) Transient sodium current at

subthreshold voltages: activation by EPSP waveforms. Neuron 75: 1081-1093.
Clayton EC, Rajkowski J, Cohen JD, Aston-Jones G. (2004) Phasic activation of monkey locus coeruleus neurons by simple decision in a forced-choice task. J. Neurosci. 24: 9914-9920.
D'Angelo E, De Fillippi G, Rossi P, Taglietti V. (1998) Ionic mechanism of electroresponsivieness in cerebellar granule cells implicates the action of a persistent sodium current. J Neurophysiol. 80: 493-503.
Del Negro CA, Koshiy N, Butera RJ, Smith JC. (2002) Persistent sodium current, membrane properties and bursting behavior or pre-botzinger complex inspiratory neurons in vitro. J. Neurophysiol. 88: 2242-2250.
Gutfreund Y, Yarom Y, Segev I. (1995) Subthreshold oscillations and resonant frequency in guinea-pig cortical neurons: physiology and modeling. J. Physiol. 483: 621-640.
Florin-Lechner SM, Druhan JP, Aston-Jones G, Valentino RJ. (1996) Enhanced norepinephrine release in prefrontal cortex with burst stimulation of the locus coeruleus. Brain Res. 742: 89-97.
Foote SL, Blomm FE, Aston-Jones G (1983) Nucleus locus coeruleus: new evidence of anatomical and physiological specificity. Physiol Rev 63: 844-914.
Foote SL, Aston-Jones G, Bloom FE. (1980) Impulse activity of locus coeruleus neurons in awake rats and monkeys is a function of sensory stimulation and arousal. Proc. Natl. Acad. Sci. USA 77: 3033-3037.
Hobson JA, McCarley RW, Wyzinski P (1975) Sleep cycle oscillation: reciprocal discharge by two brainstem neuronal groups. Science 189: 55-58.
Hu H, Vervaeke, K, Storm JF. (2002) Two forms of electrical resonance at theta frequencies, generated by M-current, h-current and persistent-Na^+ current in rat hippocampal pyramidal cells. J. Physiol. 545: 783-805.
Ishimatsu M, Williams JT. (1996) Synchronous activity in locus coeruleus results from dendritic interactions in pericoerulear regions. J Neurosci **16**:5196-204.
Khaliq ZM, Bean BP. (2010) Pacemaking in dopaminergic ventral tegmental area neurons: depolarizing drive from background and voltage-dependent sodium conductances. J. Neurosci. 30(21): 7401-7413.
Kononenko NI, Shao LR, Dudek FE. (2004) Riluzole-sensitive slowly inactivation sodium current in rat suprachiaasmatic nucleus neurons. J. Neurophysiol. 91: 710-718.
Min MY, Wu YW, Shih PY, Lu HW, Lin CC, Wu Y, Li MJ, and Yang HW (2008) Physiological and morphological properties of, and effect of substance P on, neurons in the A7 catecholamine cell group in rats. Neuroscience 153: 1020-1033.
Min MY, Wu YW, Shih PY, Lu HW, Wu Y, Hsu CL, Li MJ, and Yang HW (2010) Roles of A-type potassium currents in tuning spike frequency and integrating

synaptic transmission in noradrenergic neurons of the A7 catecholamine cell group in rats. Neuroscience 168:633-645.

Pennartz CMA, Bierlaagh MA, Geurtsen AMS. (1997) Cellular mechanisms underlying spontaneous firing in rat suprachiasmatic nucleus: involvement of slowly inactivating component of sodium current. J. Neurosci. 78: 1811-1825.

Stafstrom CE (2007) Persistent sodium current and its role in epilepsy. Epilepsy Currents 7(1): 15-55.

Swanson LW (1976) The locus coeruleus: a cytoarchitectonic, Golgi and immunohistochemical study in the albino rat. Brain Res. 110: 39-56.

Verheugen JA, Vijverberg HP, Oortigiesen M, Cahalan MD. (1995) Voltage-gated and Ca^{2+}-activated K^{+} channels in intact human T lymphocytes. Noninvasive measurements of membrane currents, membrane potential, and intracellular calcium. J. Gen. Physiol. 105: 765-794.

Verheugen JA, Fricker D, Miles R. (1999) Noninvasive measurements of the membrane potential and GABAergic action in hippocampal interneurons. J. Neurosci. 19: 2546-2555.

White JA, Klink R, Alonso A, Kay AR. (1998) Noise from voltage-gated ion channels may influence neuronal dynamics in the entorhinal cortex. J. Neurophysiol. 80: 262-269.

Williams SR, Stuart GJ. (1999) Mechanisms and consequences of action potential burst firing in rat neocortical pyramidal neurons. J. Physiol. 521: 467-482.

Figure and legends

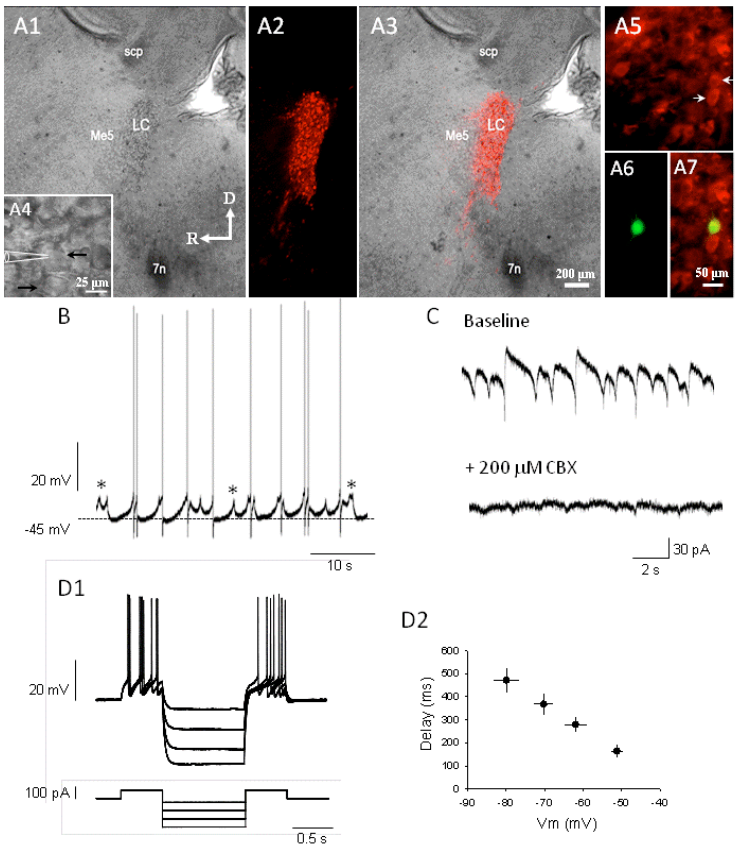

Figure 1. Identification of LC neurons in saggital brainstem slice. ***A1 & A4*** are bright file images showing a paraformadehyde fixed slice at low (A1) and high (A2) magnification. ***A2*** & ***A3*** are fluorescent of IHC (A2) and merged (A3 with A1) images. Note dense of TH-ir neurons in LC. ***A5-A7*** are fluorescent images of IHC (A5), biocytin histochemistry (A6) and merge of IHC and biocytin (A7) at high magnification. Arrows (white) mark two TH-ir neurons that are also marked in A4 (see arrows); one of them (top) was recorded and filled with biocytin (see A6 & A7). Abreactions: 4th, the 4th ventricle; 7n, 7th nerve; Me5, mesencephalic trigeminal nucleus; *scp*: superior cerebellar peduncle. Large arrows in A1 indicate slice orientation (D: dorsal; R: rostral) and the

scale (500 μm). ***B-C***. Representative current (B) and voltage (C) clamp recording form a TH-ir neurons show spontaneous AP; voltage oscillations (see asterisks in B) and the underlying membrane currents (top trace in C), which was blocked upon subsequent application of 200 μM CBX, a gap junction blocker (bottom trace). ***D***. Representative current clamp recording shows membrane voltage (Vm) responses (top traces) to current injection paradigm shown in bottom traces (D1) and the summarized results (D2). Note hyperpolarization of Vm upon current pulse injection delayed action potential (see arrow in D1) in Vm-dependent manner (D2).

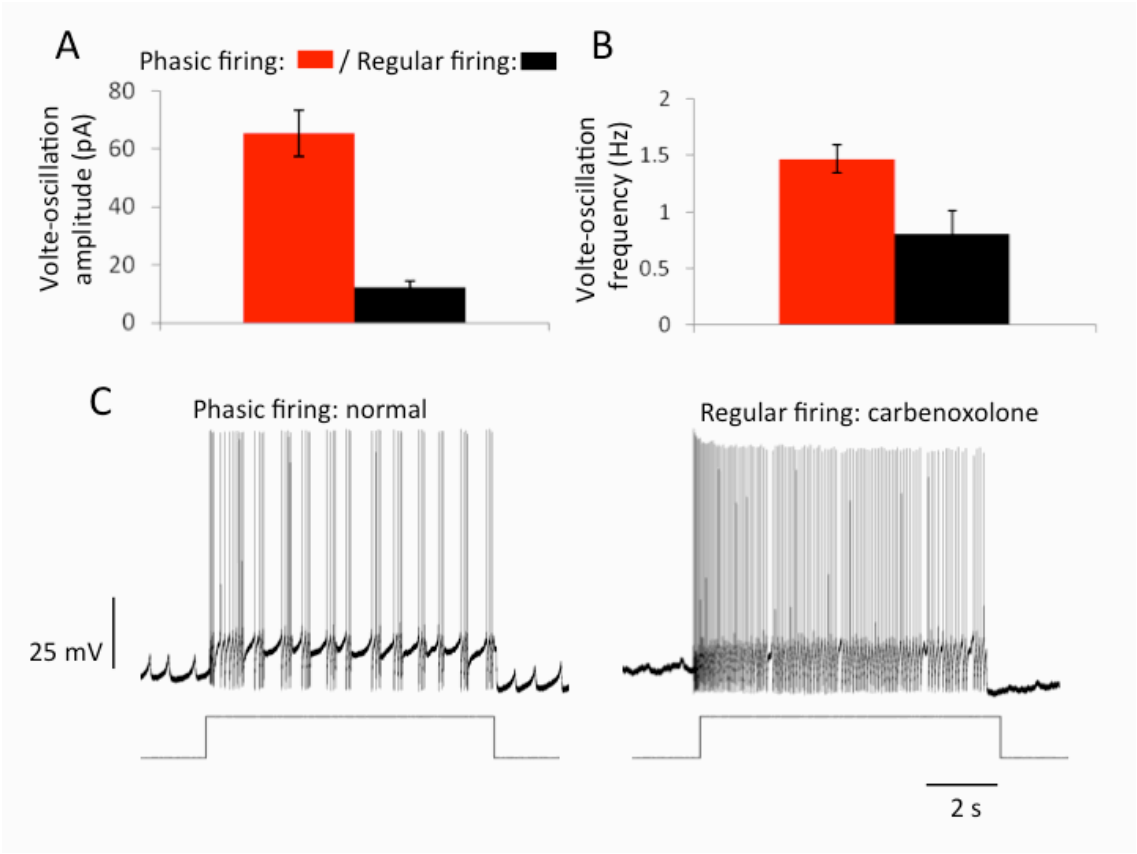

Figure 2. *The impact of gap junction mediated-oscillation to firing pattern*
A. The comparison of average oscillation amplitude (A) and frequency (B) between phasic and regular firing groups. The difference was significant at $p< 0.0.1$ level in both cases using Mann-Whiney *U*-test. C. Typical recording from a phasic firing LC neurons in normal condition (left). Note that it shifted to regular firing after of carbenoxolone.

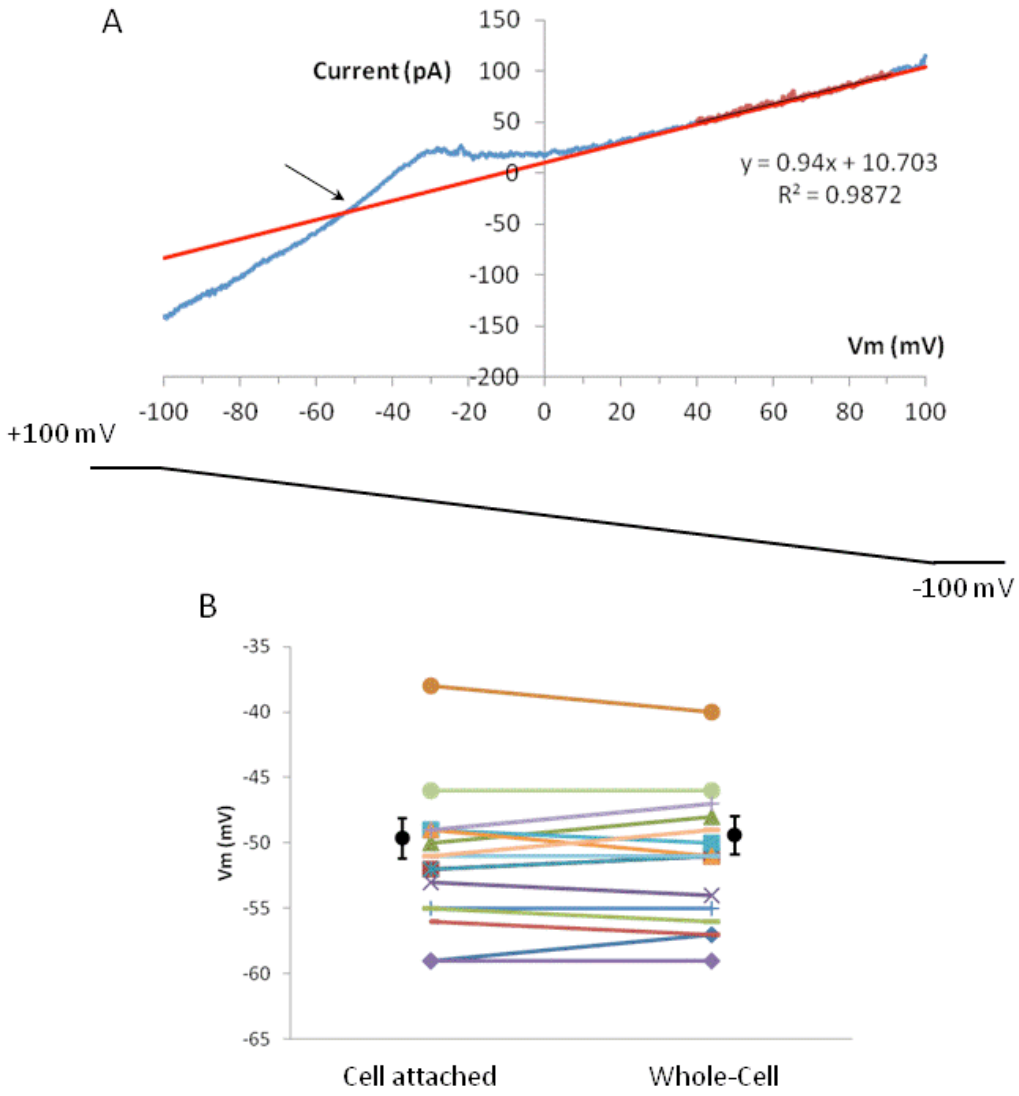

Figure 3. *Noninvasive measurements of the membrane potential*
A. A representative example of K^+ current (top) evoked by voltage-ramp from +100 to -100 mV (bottom) in cell-attached recording. Note the measured reversal potential, the physiological membrane potential, as marked by the arrow. *B*. The average of estimated membrane potential from among 17 cells using cell-attached (noninvasive) and subsequent in whole cell recording.

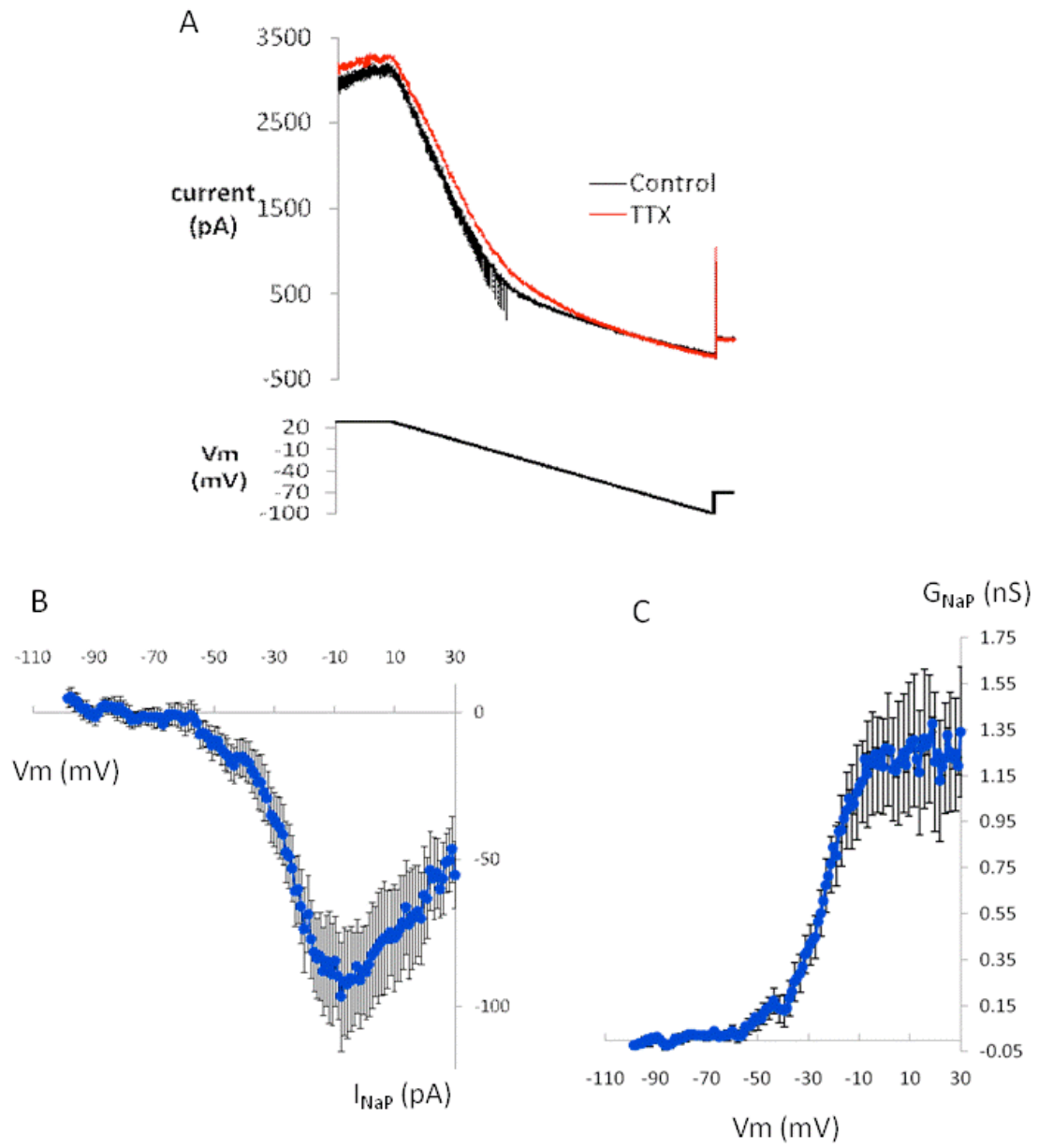

Figure 4. *I_{NaP} in LC neurons*

A. Represent recording of membrane the currents (top) elicited by 10 mV/s ramp from +30 mV to -100 mV (bottom) in normal condition (top: black trace) and subsequent application of 1 μM TTX (top: red trace) into the bath medium. *B.* Voltage-I relationship of I_{NaP} by subtracting membrane currents recorded in TTX application from that in normal condition. The results are summarized from 12 LC neurons. C. Conversion of voltage-I relationship to voltage-conductance relationship.

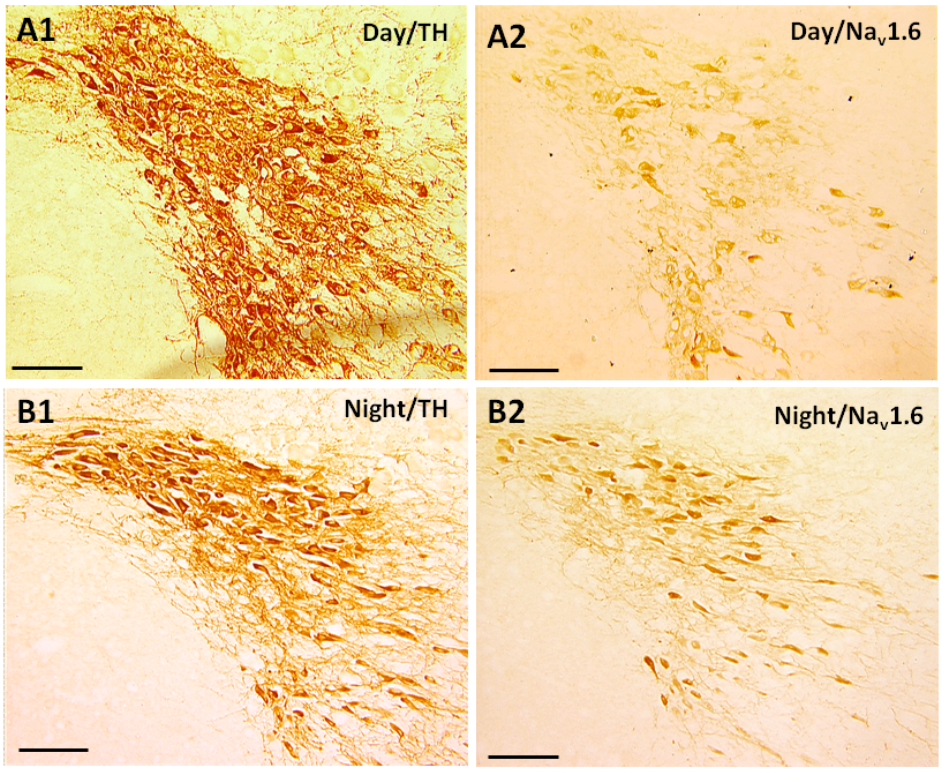

Figure 5. Representative photographs showing double-immunostaining results. An increased number of LC neurons at night time are labeled with anti-TH and anti- $Na_v1.6$ antibodies (B1 & B2), while most cells are only labeled with anti-TH antibodies (A1 & A2) at day time. Scale bar= 100 μm.

國科會補助專題研究計畫出席國際學術會議心得報告

計畫編號	NSC-100-2320-B-040-010-MY3		
計畫名稱	電位依賴型鈉離子電流在藍斑核正腎上性素神經元節律性自發放電行為之探討		
出國人員姓名	楊琇雯	服務機構及職稱	中山醫學大學 教授
會議時間	2014 年 7 月 5 日 至 2014 年 7 月 9 日	會議地點	義大利 米蘭
會議名稱	第 9 屆歐洲神經科學大會 The 9th FENS Forum of Neuroscience		
發表題目	1. 長期出生前暴露 CITALOPRAM 減少雄性而非雌性大鼠藍斑核神經元 $GABA_B$ 受器功能 Chronic perinatal citalopram exposure reduces $GABA_B$ receptor functionality in locus coeruleus neurons in male but not female rats. 2. $GABA_B$ 受器在大鼠藍斑核的細胞內分佈 Subcellular localization of $GABA_B$ receptor in rat locus coeruleus.		

一、參加會議經過及與會心得

2014年第9届歐洲神經科學大會，於7月5至9日在義大利米蘭國際會議中心舉行為期五天的會議。會議中安排有Plenary lectures、Special lectures與Symposiums，因此不論是新的正在進行中的研究（如壁報論文）、重要研究主題的回顧與未來展望（symposium會議），或者傑出學者的經典研究（如plenary lectures、special lecture），都能提供與會者非常多的選擇，因此是一個安排很好的會議。其內容涵蓋所有現今國際神經科學研究的所有重要領域，包括：Adjusting brain circuits for learning and memory, Neuromodulation of brain states, Explorations of a simple visual cortex, Building connections: RNA-based mechanism of axon guidance, Optogenetic tools for controlling neural activity with light, Cell biology of the neuron: membrane lipid dynamics in the regulation of synaptic function, Processing of correlated synaptic input by dendrites, Mitochondrial and presynaptic dysfunction in Parkinson′s disease, Neural dynamics in visual cortex during learning等。本人在此次會議中有幸聆聽許多演講，以及有機會與其他與會學者暢談。其中最令人印象深刻是“Synaptkc structure and function illuminated by fluorescence and electron microscopy”，“Neurobiological and neurogenetic bases of the link between sleep, stress and depression”與“Development and function of GABA circuits”這三場symposiums，以及“Processing of correlated synaptic input by dendrites”與 “Neural dynamics in visual cortex during learning”這兩場special lectures。我們的壁報“Chronic perinatal citalopram exposure reduces $GABA_B$ receptor functionality in locus coeruleus neurons in male but not female rats”、“Subcellular localization of $GABA_B$ receptor in rat locus coeruleus”，在星期一下午展出。有來自台灣、日本、美國、英國、法國學者前來觀看我們的壁報，並且提出一些寶貴的意見。

參加這次第 9 届歐洲神經科學大會，能親自聆聽神經科學領域中大師級的演講，以及經典的研究與最新的發現，也有機會與來自世界各地的學者專家交換心得，這些都要感謝學校的支持與科技部經費補助。

二、發表論文摘要

ABSTRACT

Poster Instructions

Back

Title	**CHRONIC PERINATAL CITALOPRAM EXPOSURE REDUCES GABAB RECEPTOR FUNCTIONALITY IN LOCUS COERULEUS NEURONS IN MALE BUT NOT FEMALE RATS.** **Room: Poster Area - Session: B26 - Abstract Number: FENS-2641 - Poster Board Number: B014**
Poster No:	B014
Presenter:	H. Yang
Author(s):	**H. Yang**(1), H.Y. Wang(2), R. Chen(2), M. Min(2)
Affiliation(s):	(1)Department of Biomedical Sciences, Chung Shan Medical University, Taichung, Taiwan ; (2)Life Science, National Taiwan University, Taipei, Taiwan
Session:	B26: Poster Session - Neurotransmitters and signalling molecules - GABA and glycine Poster boards: B001-014
Date:	Monday - July 07, 2014 14:30 - 15:30
Location:	Poster Area
Subtopic:	B.1.b GABA and glycine
Topic:	B.1 Neurotransmitters and signalling molecules
Theme:	B. Excitability, synaptic transmission, network functions

The selective serotonin reuptake inhibitors (SSRIs), including citalopram (CTM), are preferred for antidepressant treatment because of their low toxicity and wide therapeutic index. Nevertheless, in dorsal raphe neurons chronic treatment with SSRI (fluoxetine) leads to reduce levels of somatodentritic $GABA_B$ receptors ($GABA_B$Rs) (Cornelisse et al. 2007, *J Neurophysiol* **98**:196). Here we examined whether a similar downregulation of $GABA_B$R functionality also occurred in locus coeruleus (LC) neurons. We observed a significantly reduction by 28.29±4.7 % of baclofen induced currents in LC neurons in CTM-treated male rats, but no effect was seen in female rats. Consistent with this observation, the $GABA_B$R mediating tonic current was significantly decreased by a similar extent (29.45±6.2 %) in CTM-treated male rats compared to saline-treated male rats, but no effect was seen in female rats. In slices from CTM-treated male rats, the baseline SFR (spontaneous firing rate) of the LC neurons was 0.56±0.01 Hz, significantly higher than that of 0.29±0.02 Hz in slices from saline-treated male rats. Removing the $GABA_B$R tonic current by adding CGP54626 to the bath reduced the difference in the SFR of LC neurons between CTM-treated and saline-treated male rats. Together, our results show that, in male rats with chronic perinatal CTM exposure, there are less functional (surface) $GABA_B$Rs, and thus a lower tonic inhibition than in saline-treated rats. This abnormal $GABA_B$R functionality might partially account for the higher SFR of LC neurons seen in the male CTM-treated rats (also see Darling et al., 2010, *J Neurosci* **31**:16709).

ABSTRACT

Poster Instructions

Back

Title	**SUBCELLULAR LOCALIZATION OF GABAB RECEPTOR IN RAT LOCUS COERULEUS.** **Room: Poster Area - Session: B26 - Abstract Number: FENS-1289 - Poster Board Number: B005**
Poster No:	B005
Presenter:	Z. Kuo
Author(s):	**Z. Kuo**(1), Y. Fu(2), M. Min(1), H. Yang(3)
Affiliation(s):	(1)Department of Life Science, National Taiwan University, Taipei, Taiwan ; (2)Department of Anatomy and Cell Biology, National Yang-Ming University, Taipei, Taiwan ; (3)Department of Biomedical Science, Chung-Shan Medical University, Taichung, Taiwan
Session:	B26: Poster Session - Neurotransmitters and signalling molecules - GABA and glycine Poster boards: B001-014
Date:	Monday - July 07, 2014 13:30 - 14:30
Location:	Poster Area
Subtopic:	B.1.b GABA and glycine
Topic:	B.1 Neurotransmitters and signalling molecules
Theme:	B. Excitability, synaptic transmission, network functions

Locus coeruleus (LC) consisting of noradrenergic neurons is the major norepinephrine (NE) supply to the forebrain. One of the well known functions of LC neuron has been its role in regulating the wakefulness/arousal level of the brain and several studies have shown that GABA appears to be an important player in this regulation. It has been shown that about 2/3 of synapses on LC neurons are GABAergic and that ambient GABA levels in the LC are significantly higher during REM/non-REM sleep than during wakefulness. To further explore the GABA control of LC neuron excitability, here we examined the subcellular distribution of $GABA_B$ receptors ($GABA_BR$) using immunehistochemistry method at electron microscopy level. We observed that $GABA_BR$-immunoreactive (ir) gold particles

located at the pre- and postsynaptic elements of both symmetric and asymmetric synapses on LC neurons. For both pre- and postsynaptic elements, the majority of $GABA_BR$-ir gold particles are at peri-/extrasynaptic sites. In addition, some $GABA_BR$-ir gold particles were found on the membrane of cytosolic organelles, some of which located beneath the synaptic or perisynaptic active zone. These observations together with our previous electrophysiological study suggest that ambient GABA can continuously activate peri-/extrasynaptic $GABA_BRs$ and exert tonic inhibition of LC neurons. Verifying the extent of this $GABA_BR$-mediated tonic inhibition can effectively tune the frequency of spontaneous firing of LC neurons.

科技部補助計畫衍生研發成果推廣資料表

日期:2014/11/10

科技部補助計畫	計畫名稱: 電位依賴型鈉離子電流在藍斑核正腎上性素神經元節律性自發放電行為之探討
	計畫主持人: 楊琇雯
	計畫編號: 100-2320-B-040-010-MY3　　學門領域: 生理

無研發成果推廣資料

100 年度專題研究計畫研究成果彙整表

計畫主持人：楊琇雯	計畫編號：100-2320-B-040-010-MY3
計畫名稱：電位依賴型鈉離子電流在藍斑核正腎上性素神經元節律性自發放電行為之探討	

成果項目			量化			單位	備註（質化說明：如數個計畫共同成果、成果列為該期刊之封面故事...等）
			實際已達成數（被接受或已發表）	預期總達成數(含實際已達成數)	本計畫實際貢獻百分比		
國內	論文著作	期刊論文	0	0	100%	篇	
		研究報告/技術報告	0	0	100%		
		研討會論文	0	0	100%		
		專書	0	0	100%		
	專利	申請中件數	0	0	100%	件	
		已獲得件數	0	0	100%		
	技術移轉	件數	0	0	100%	件	
		權利金	0	0	100%	千元	
	參與計畫人力（本國籍）	碩士生	0	0	100%	人次	
		博士生	0	0	100%		
		博士後研究員	0	0	100%		
		專任助理	0	0	100%		
國外	論文著作	期刊論文	0	0	100%	篇	
		研究報告/技術報告	0	0	100%		
		研討會論文	1	0	100%		第 9 屆歐洲神經科學年會研討會論文
		專書	0	0	100%	章/本	
	專利	申請中件數	0	0	100%	件	
		已獲得件數	0	0	100%		
	技術移轉	件數	0	0	100%	件	
		權利金	0	0	100%	千元	
	參與計畫人力（外國籍）	碩士生	0	0	100%	人次	
		博士生	0	0	100%		
		博士後研究員	0	0	100%		
		專任助理	0	0	100%		

其他成果 (無法以量化表達之成果如辦理學術活動、獲得獎項、重要國際合作、研究成果國際影響力及其他協助產業技術發展之具體效益事項等，請以文字敘述填列。)	無

	成果項目	量化	名稱或內容性質簡述
科教處計畫加填項目	測驗工具(含質性與量性)	0	
	課程/模組	0	
	電腦及網路系統或工具	0	
	教材	0	
	舉辦之活動/競賽	0	
	研討會/工作坊	0	
	電子報、網站	0	
	計畫成果推廣之參與（閱聽）人數	0	

科技部補助專題研究計畫成果報告自評表

請就研究內容與原計畫相符程度、達成預期目標情況、研究成果之學術或應用價值（簡要敘述成果所代表之意義、價值、影響或進一步發展之可能性）、是否適合在學術期刊發表或申請專利、主要發現或其他有關價值等，作一綜合評估。

1. 請就研究內容與原計畫相符程度、達成預期目標情況作一綜合評估

■達成目標

□未達成目標（請說明，以 100 字為限）

□實驗失敗

□因故實驗中斷

□其他原因

說明：

2. 研究成果在學術期刊發表或申請專利等情形：

論文：□已發表 □未發表之文稿 ■撰寫中 □無

專利：□已獲得 □申請中 ■無

技轉：□已技轉 □洽談中 ■無

其他：（以 100 字為限）

3. 請依學術成就、技術創新、社會影響等方面，評估研究成果之學術或應用價值（簡要敘述成果所代表之意義、價值、影響或進一步發展之可能性）（以 500 字為限）

LC 神經元對大腦有非常廣泛的正腎上腺素纖維投射，因此在大腦功能狀態的調節上扮演極重要的角色，包括睡眠-清醒狀態與痛覺傳遞的調節。過去的研究顯示，LC 神經元具有節律性自發放電的行為，並且其頻率與型式特徵具有日週期性的變化；此節律性自主放電的行為的日週期性變化，一般認為與 LC 神經元調節大腦的睡眠-清醒狀態功能息息相關。不過，現今的神經細胞學知識對於LC神經元如何節律性的自主放電？什麼樣的機轉可以造成LC神經元自主節律放電的頻率與型式改變而改變？又如何具有日週期性？以上等等問題的了解都相當缺乏。除此之外，神經細胞是否具有節律性自主放電的能力，其細胞膜上是否表現低活化閾值的離子通道蛋白是主要的關鍵。最近的許多研究顯示，許多具有節律性自主放電能力的中樞神經細胞有表現 INaP 通道，因此本計畫透過研究具低活化閾值 (low threshold) 與能持續活化(persistently activated) 的膜電位依賴型 (voltage-dependent) 鈉離子電流 (persistent sodium current；簡稱 INaP) 在藍斑核的表現與功能分析，以回答在這個領域中尚未解決的重要議題。我們的研究成果顯示 LC 神經元有表現 INaP，並且 INaP 活化閾值膜電位低靜止膜電位。除此之外，最近的實驗發現，給予選擇性 INaP 抑制劑，riluzole，可抑制 LC 神經元自發放電行為。我們也有發現

gap junction 與 INaP 之間有互相作用，因為電位震盪與 LC 神經元自發放電之間有所關聯。這個發現強烈的建議 INaP 可能在 LC 神經元自發性放電上扮演一個重要的角色。除此之外，我們發現 Nav1.6 離子通道的表現量有 24 小時日週期性的變化，因此推測 Nav1.6 離子通道在調控藍班核正腎上性素神經元動作電位放射頻率上扮演重要的角色。我們堅信本計劃所完成的工作，除了適合發表在學術期刊之外，更能使我們了解藍班核對大腦清醒與睡眠等功能狀態週期的調節，也可使我們更了解中樞神經系統如何透過 Nav 通道的角色來調整神經細胞的放電行為，進而調整生理的功能。